

Response of soil nitrogen retention to the interactive effects of soil texture, hydrology, and organic matter

Michael J. Castellano,¹ David Bruce Lewis,² and Jason P. Kaye³

Received 7 May 2012; revised 11 December 2012; accepted 15 December 2012.

[1] Advances in nitrogen (N) saturation and retention theories have focused on soil organic matter (SOM) biogeochemistry in the absence of dynamic soil hydrology. Here we exploit two soil types with contrasting textures that span a hillslope gradient to test hypotheses that suggest N saturation symptoms are regulated by the interactive effects of soil texture, OM, and hydrology on N retention capacity (maximum pool size) and N retention kinetics (N retention rate). Down the hillslope gradient, soil solution nitrate (NO₃) concentrations sampled with lysimeters increased, while ¹⁵NO₃-N retention decreased. Landscape location (upland, hillslope, and toeslope) and soil type interacted to affect soil solution NO₃ concentrations so that the downslope increase in NO₃ was greater in sandy versus silty soils. These patterns manifest despite a downslope increase in soil organic carbon (SOC) and C/N ratios. A positive correlation between saturated hydraulic conductivity and soil solution NO₃ sampled in zero-tension lysimeters during precipitation events suggested that high hydraulic conductivity promotes periodic rapid NO₃ transport at rates that exceed retention kinetics. The downslope increase in soil solution NO₃ in spite of a concomitant increase in SOC and C/N ratios provides an important contrast with previous N saturation research that highlights negative correlations between SOM C/N ratios and NO₃ concentrations and suggests NO₃ transport along connected hillslope flow paths may overwhelm stoichiometric sinks for inorganic N retention in SOM. Our results reveal important gaps in N retention theory based on SOM biogeochemistry alone and demonstrate how coupled biogeochemical and hydrological models can improve predictions of N saturation, particularly when considering periodic advective NO₃ transport in the vadose zone. We show that in coarse-textured soils, low capacity for protection of SOM N by association with fine mineral particles interacts with rapid hydrological flushing of NO₃ to enhance the expression of ecosystem N saturation symptoms.

Citation: Castellano, M. J., D. B. Lewis and J. P. Kaye (2013), Response of soil nitrogen retention to the interactive effects of soil texture, hydrology, and organic matter, *J. Geophys. Res. Biogeosci.*, 118, doi:10.1002/jgrg.20015.

1. Introduction

[2] Fossil fuel combustion and agricultural activities have increased atmospheric nitrogen (N) deposition. Terrestrial N deposition can lead to symptoms of ecosystem N saturation, including soil acidification, increasing nitrate (NO₃) concentrations, vegetation mortality, and N loss to atmospheric and aquatic environments [Aber *et al.*, 1989]. However, the expression of N saturation symptoms can be highly variable

among ecosystems despite similar N inputs. Some ecosystems express N saturation symptoms after small, short-term N additions [Pregitzer *et al.*, 2004], while other ecosystems efficiently retain large N additions in soil organic matter (SOM) sinks that resist mineralization [Kaye *et al.*, 2002; Magill *et al.*, 2000].

[3] Given similar N inputs, ecosystems vary in how quickly they express N saturation symptoms due to either variation in maximum N sink size (capacity) or variation in the rate at which inorganic N can be retained (kinetics) [Lovett and Goodale, 2011]. Thus, there are two routes to N saturation: capacity saturation (N sinks are filled) and kinetic saturation (N input rate exceeds N retention rate). The dominant ecosystem N sink is SOM, and most N saturation symptoms are manifest as a result of kinetic N saturation [Schlesinger, 2009].

[4] Although it is well known that biological and hydrological processes account for variation in N saturation and retention [Gu and Riley, 2010; Maggi *et al.*, 2008], much empirical research has exclusively focused on SOM biogeochemistry or watershed hydrology [Mitchell, 2001]. As a

All Supporting Information may be found in the online version of this article.

¹Department of Agronomy, Iowa State University, Ames, Iowa, USA.

²Department of Integrative Biology, University of South Florida, Tampa, Florida, USA.

³Department of Ecosystem Science and Management, The Pennsylvania State University, University Park, Pennsylvania, USA.

Corresponding author: M. J. Castellano, Department of Agronomy, Iowa State University, Ames, IA 50014, USA. (castellanomichaelj@gmail.com)

result, ecosystem N saturation has been characterized by a variety of biological and hydrological symptoms. Biological studies have focused on surface SOM properties and the biological demand for N; biological symptoms of N saturation include low SOM carbon (C)/N ratios, low efficiency of inorganic N retention in SOM, and low microbial N demand, as well as high net nitrification, high soil solution NO_3 concentrations, and high NO_3 leaching [Emmett, 2007; Lewis and Kaye, 2011; Lovett et al., 2002; Zogg et al., 2000]. By contrast, hydrological studies have focused on the temporal pattern and magnitude of ecosystem NO_3 export at soil pedon and watershed scales [Dittman et al., 2007; van Verseveld et al., 2008]. Large NO_3 export with little seasonal variation is symptomatic of capacity N saturation (N sinks are filled) [Lovett et al., 2000]. Alternatively, increased NO_3 concentrations and export during periodic episodes of high water flow are symptomatic of kinetic N saturation (N transport rates exceed N retention kinetics). In these situations, rapid soil water flow can overwhelm the kinetics of biological NO_3 immobilization in SOM sinks [Evans et al., 2008]. Evidence of this process includes observations of NO_3 flushing, a pattern that is manifest during intense precipitation events and characterized by rapid NO_3 transport from nutrient-rich surface soils through subsoils to watershed discharge [Creed and Band, 1998; Pionke et al., 1996; van Verseveld et al., 2008].

[5] We hypothesize that the effects of soil texture on SOM stabilization and hydrology interact to regulate biological N demand and hydrological N transport. The capacity to retain inorganic N inputs in SOM sinks is affected by soil texture [Castellano et al., 2012; Kaye et al., 2002]. Physicochemical association of SOM with fine mineral particles (silt and clay) can protect N from microbial mineralization, thereby maintaining high microbial N demand [Sollins et al., 1996]. A lower fine particle surface area in sandy soils limits SOM protection from mineralization, thereby decreasing the potential for inorganic N transfer to and retention in SOM [Castellano et al., 2012; Six et al., 2002]. However, inorganic N inputs must be microbially transformed to organic N compounds before they can be retained in SOM pools that resist mineralization [Norton and Firestone, 1996; Zogg et al., 2000]. Rapid hydrological inputs of inorganic N in coarse-textured soils with high hydraulic conductivity could overwhelm microbial immobilization processes, limiting the retention of inorganic N in SOM [Evans et al., 2008]. Consistent with this hypothesis, N retention in sandy soils is often low, particularly during rainfall events [Lajtha et al., 1995; Pregitzer et al., 2004].

[6] As ecosystem N inputs accumulate, soil texture also affects the pattern of N retention over time. Sandy soils have less SOM stabilization capacity than silty soils and the kinetics of N retention decline as capacity fills [Castellano et al., 2012; Stewart et al., 2007]. Hydrological flow paths can generate a similar pattern in space. As dissolved C and N inputs accumulate downflow paths, downflow path N sinks can approach capacity more quickly and exhibit slower retention kinetics than upflow path N sinks (despite their similar textures). Thus, hydrological processes could hasten the expression of biological N saturation symptoms by leading to a relatively rapid accumulation of N inputs in downflow path N sinks.

[7] Recent numerical models of ecosystem N dynamics incorporate interactions between microbial processes and advective transport [Gu and Riley, 2010; Maggi et al., 2008]. However, models have limited ability to accurately characterize large N fluxes during short periods of time, such as the rapid N transport that occurs during intense precipitation events. Moreover, empirical data regarding interactions between microbial and hydrological processes are scarce. Here we link SOM and hydrological processes to explain interactions between capacity and kinetic N retention controls on N saturation symptoms along hillslope flow paths in two adjacent soil types with fine and coarse textures. The two soil types supported a mature hardwood forest that had no significant differences in dominant vegetation or throughfall N deposition. We hypothesized that soils with a coarse texture would exhibit more symptoms of N saturation, including higher soil solution inorganic N concentrations and lower inorganic N retention in SOM. We further hypothesized that these N saturation symptoms would increase downslope due to the accumulation of dissolved N inputs in SOM sinks.

2. Methods

2.1. Site Description

[8] The ~0.5 ha study site is located in Abingdon, Maryland, USA (39°27'05"N, 76°16'23"W). It is part of the Chesapeake Bay, Maryland, National Oceanic and Atmospheric Association National Estuarine Research Reserve. Its mean annual temperature is 12.0 °C and mean annual precipitation is 1164 mm. Vegetation at the site is a mix of *Liquidambar styraciflua*, *Liriodendron tulipifera*, and *Quercus* spp. Tree ring analyses indicated that many individuals of the dominant tree species (*L. styraciflua*) are >110 years old (unpublished data, 2009). According to the United States Department of Agriculture Natural Resources Conservation Service (USDA NRCS), the study site contains two soil orders and three soil series: two silty Ultisols (Joppa and Elsinboro series) and a sandy Entisol (Evesboro series). We could not distinguish the two Ultisols in the field, and they are sampled as one soil type for this study. The soils are derived from quartz parent materials, but additional mineralogical data are not available. The site is part of a small catchment that spans upland to floodplain. The three soil series span upland to floodplain as well, perpendicular to the catchment drainage. The NE end of the catchment contains the Ultisols, and the SW end of the catchment contains the Entisol. The catchment gradient spans ~40 m from upland to floodplain with an ~20% slope (Figure 1). Ground-penetrating radar surveys conducted by the USDA NRCS indicated that the soils are ~1 m deep and underlain by an aquitard that influences water flow laterally downslope (unpublished data, 2009). The aquitard was visually confirmed to be a lithified paleosol with low hydraulic conductivity likely dating to the Cretaceous (T. White, pers. comm.). The effect of the paleosol on water flow was apparent at the floodplain intersection of the paleosol and soil surface where water regularly seeped (supporting information).

2.2. Sampling Approach

[9] We established eight transects that spanned upland to floodplain, perpendicular to the catchment drainage (Figure 1).

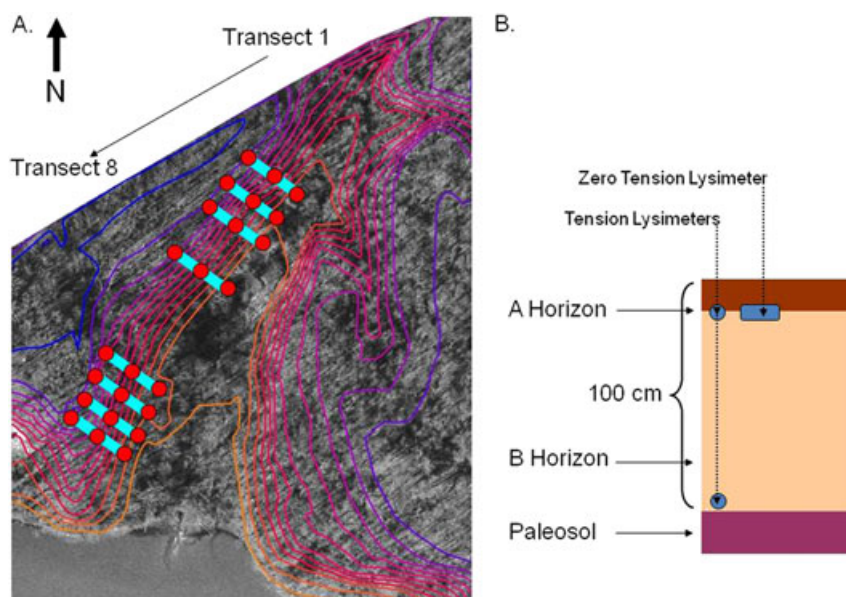


Figure 1. (a) Map of the research location. Contour lines are 1 m. Blue lines represent sampling transects (40 m), and red circles represent upland, hillslope, and toeslope sampling locations on each transect. The four northern transects were in silty Ultisol soils. The four southern transects were in a sandy Entisol soil. (b) Sampling approach at the upland and hillslope transect locations. One TL and one ZTL were located at the interface of the A and B soil horizons. A second TL was located at the bottom of the B horizon. Toeslope sampling locations did not have ZTLs or B horizon TLs and only had an A horizon TL at three of the four transects within each soil type (see section 2).

Four transects were located in the Ultisols and four transects were located in the Entisol. Each transect included upland, hillslope, and toeslope sampling locations (12 sample locations in each soil order). Hillslope locations were midway between the upland and toeslope locations. We sampled soil solution and measured inorganic N retention at the 3 transect locations. In 2007 and 2008, we installed Prenart™ quartz tension lysimeters (TLs) (Denmark) at the transect locations. At all upland and hillslope locations, TLs were inserted at the interface between the A and B soil horizons (12–15 cm) as well as at the bottom of the B soil horizon (85–100 cm below the soil surface). At the toeslope locations, TLs were only inserted at the A/B soil horizon interface (shallow depth) on three of the four transects in each soil type (6 of 8 total toeslope locations) due to equipment limitations. We also installed polyvinyl chloride zero-tension lysimeters (ZTLs) at the interface between the A and B soil horizons at all upland and hillslope locations (to correspond with shallow TLs). We did not install ZTLs at toeslope locations because the water table reached the A horizon during intense precipitation events, confounding our ability to sample water moving vertically and laterally down the hillslope. Nevertheless, all toeslope locations were above water seeps and exhibited no redoximorphic features or alluvial discontinuities. TLs were fabricated from a porous quartz material; a vacuum (−70 kPa) was placed on the lysimeter for ~18 h during which a sample was collected. The samples were not collected during rain events and thus sampled soil solutions that were not moving rapidly. By contrast, ZTLs “catch” water that is advectively transported into the collection area that was 30.0 × 9.6 cm. Our observations suggest this advective transport of soil water was limited to periods of intense or large rainfall.

[10] The lysimeters were allowed a 14 to 20 month equilibration period during which they were sampled every 2–4 weeks. These samples were discarded. From 1 October 2008 to 5 November 2009 (after the equilibration period), we sampled all TLs every 1–4 weeks, with more frequent sampling during times when all lysimeters were collecting samples (February–June). We sampled all ZTLs after intense precipitation events. Our first lysimeter samples were collected in December 2008 due to dry soil conditions during October–November that did not produce samples. All replicate TLs yielded samples through mid-July, and all replicate ZTLs yielded samples through August (supporting information). Some replicate lysimeters yielded samples through November 2009. Throughfall was also sampled at each transect location ($N=24$). Lysimeter and throughfall solutions were kept on ice in a cooler for <4 h, frozen, thawed, filtered (Whatman 1), and analyzed for $\text{NH}_4\text{-N}$ and $\text{NO}_3\text{-N}$ concentrations. Throughfall and TL water samples were also analyzed for oxygen isotope ratios in H_2O ($\delta^{18}\text{O}$).

[11] In August 2008, we extracted five replicate A horizon soil cores from all upland, hillslope, and toeslope transect locations (24 total locations) and five replicate B horizon soil cores from the upland and hillslope transect locations (16 of the 24 locations) using a 15 cm depth × 5 cm diameter soil core sampler and butyrate liners (i.e., 200 soil cores sampled in butyrate liners). Sampling of B horizons at the 8 locations at the bottom of the flow paths was prevented due to deep B horizon soils (>30 cm) that exhibited redoximorphic features. In a few locations, the A horizon was <15 cm deep; in these situations, we removed the B horizon portion from the soil core prior to analyses. Soil from the 200 cores was used for analyses of bulk density, soil texture, soil organic C (SOC), soil organic N (SON), C/N ratio, 2 M KCl extractable

Table 1. Mean Values for Each Soil Order, Soil Horizon, and Landscape Location ($N=4$)

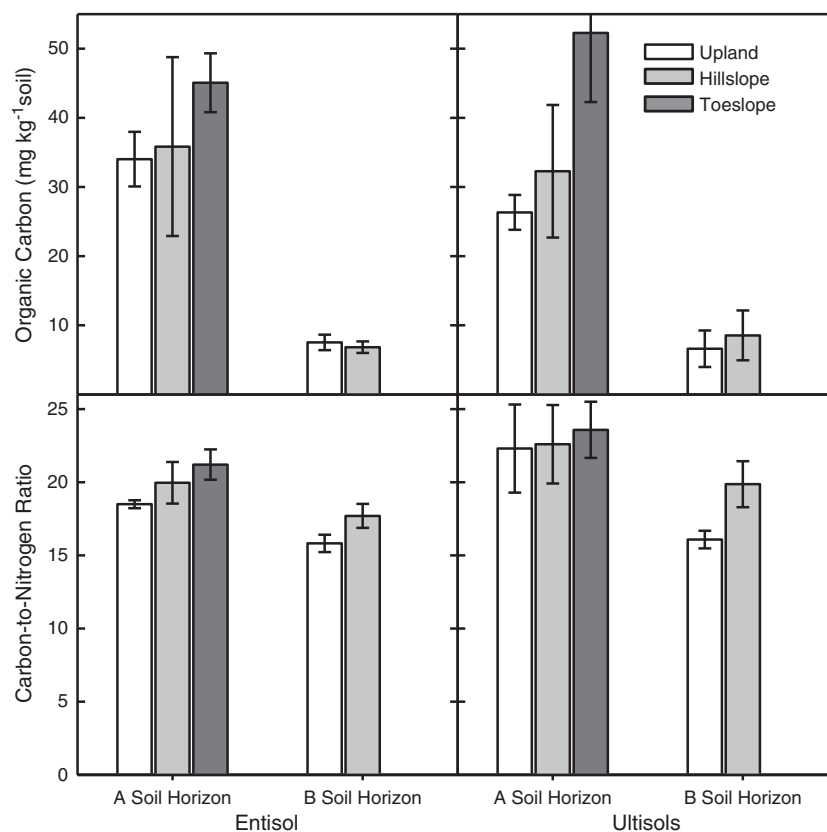
Soil Type	Landscape Location	Sand	Silt	Clay	K_s^a	Organic C	Insoluble N	C/N Ratio	pH
		(g kg ⁻¹ soil)	(g kg ⁻¹ soil)	(g kg ⁻¹ soil)	(cm s ⁻¹)	(g C kg ⁻¹ soil)	(g N kg ⁻¹ soil)		
Entisol									
A Horizon	Upland	748	181	71	0.08	34.0	1.8	18.5	3.8
	Hillslope	824	106	70	0.15	35.8	1.8	20	3.7
	Toeslope	825	103	72	-	45.1	2.1	21.2	3.9
B Horizon	Upland	769	134	97	-	7.5	0.5	15.8	4.1
	Hillslope	809	112	79	-	6.8	0.4	17.7	4.0
Ultisols									
A Horizon	Upland	544	329	127	0.02	26.3	1.2	22.3	3.9
	Hillslope	668	232	101	0.08	32.3	1.5	22.6	3.4
	Toeslope	710	192	98	-	52.3	2.2	23.6	3.9
B Horizon	Upland	583	301	116	-	6.6	0.4	16.1	4.0
	Hillslope	646	236	118	-	8.5	0.4	19.9	4.0

^aSaturated hydraulic conductivity.

Table 2. Probability ($P > F$) of Three-way ANOVA for the Effects of Independent Factors Soil Type, Soil Depth (A vs. B horizons), and Landscape Location on the Dependent Factors SOM, TL N, and Inorganic N Retention^a

Factor	ANOVA												
	Soil Texture			SOM			TLs		ZTLs		Inorganic N Retention		Hydrology
	Sand	Silt	Clay	SOC	SON	C/N	NH ₄ -N	NO ₃ -N	NH ₄ -N	NO ₃ -N	NH ₄ -N	NO ₃ -N	K_s
Soil Type	<0.0001	<0.0001	0.0024	0.5464	0.7375	0.0119	0.0006	0.0003	0.9694	0.0023	0.7537	0.2195	0.0200
Location	0.0030	0.0061	0.5121	0.0003	0.0096	0.0186	0.0004	0.0121	0.6905	0.0115	0.1737	<0.0001	0.0051
Soil Type × Location	0.4423	0.5777	0.7229	0.1650	0.2194	0.8640	0.0072	0.0648	0.8903	0.0295	0.4665	0.7181	0.3340
Soil Depth	0.7852	0.5060	0.3123	<0.0001	<0.0001	<0.0001	0.1097	0.0009	-	-	0.0023	0.0100	-
Soil Type × Depth	0.9418	0.8552	0.5416	0.1967	0.0385	0.1276	0.2100	0.0218	-	-	0.1640	0.4661	-

^aThe ZTLs were only installed at the shallow depth in upland and hillslope locations; thus, the results represent two-way ANOVA with the independent factors soil type and landscape location.


Figure 2. SOM properties. Data represent the mean and standard error ($N=4$). Soil C/N ratio is reported on a mass basis. See Table 2 for statistics.

NH₄ and NO₃ pool sizes, and 3 day transfer of ¹⁵NH₄-N and ¹⁵NO₃-N to soil pools that were not extractable with 2 M KCl.

[12] On the August 2008 sampling date, using the five intact soil cores collected at each transect location, we injected two cores with ¹⁵NH₄Cl and two cores with K¹⁵NO₃, with the fifth core reserved to determine ¹⁵N natural abundance. Soil cores from the A horizon were injected with 0.75 mg of 70.4% APE ¹⁵NH₄Cl-N and 0.5 mg of 60.2% APE K¹⁵NO₃-N, while B horizon soil cores were injected with 0.6 mg of 70.4% APE ¹⁵NH₄Cl-N and 0.4 mg of 60.2% APE K¹⁵NO₃-N. Masses of NH₄ and NO₃ applications were selected to limit increases in background concentrations while permitting detection of the ¹⁵N tracer in relatively large SOM N pools. On average, these ¹⁵N additions increased the A horizon NH₄ pool by 17%, the B horizon NH₄ pool by 26%, the A horizon NO₃ pool by 26%, and the B horizon NO₃ pool by 35%. All N applications were delivered in injections of deionized water that totaled 5 mL of solution per soil core and increased soil moisture by ~1.7%. Cores were capped at both ends; the top cap was perforated to allow for gas exchange. Fifteen minutes after injection, the ambient core, one ¹⁵NH₄Cl-injected soil core, and one K¹⁵NO₃-injected soil core were extracted for NH₄ and NO₃ by reciprocal shaking for 2 h in a 2 M KCl solution at an m/v ratio of 1:5 (soil/KCl). After shaking, the solution was filtered (pre-leached Whatman 1) for determination of NH₄-N and NO₃-N on a flow injection spectrophotometer. Initial NH₄-N and NO₃-N pools (mass N/mass dry soil, <2 mm) were determined from the mean value of these three soil cores. The remaining ¹⁵NH₄Cl-injected soil core and K¹⁵NO₃-injected

soil core were left in the field to incubate for 3 days, and then NH₄-N and NO₃-N were extracted using the above procedure. The masses of ¹⁵NH₄-N and ¹⁵NO₃-N that remained in the residual extracted soil after 3 days were measured; we assumed these represented N that was immobilized in SOM during the 3 day incubation. We calculated the 3 day transfer of ¹⁵NH₄-N and ¹⁵NO₃-N to SOM as a fraction of the mean initial NH₄-N and NO₃-N pools that were labeled with ¹⁵N and determined from the cores extracted at 15 min.

[13] In August 2008, we sampled one 26.5 cm depth × 9 cm diameter soil core from the upland and hillslope transect locations ($N=16$) for laboratory analysis of saturated hydraulic conductivity (K_s). Samples were collected to test hypotheses regarding ZTL N concentrations and thus not collected at toeslope locations where ZTLs were absent. Samples were refrigerated at 4 °C for approximately 1 week for lab analyses. The constant head method was used to determine K_s [Klute and Dirksen 1986] with minor modifications as suggested by Walker [2008]. Prior to analysis, the cores were saturated in a solution of de-aired 0.005 M calcium sulfate to minimize soil flocculation. Air was removed from the solution by bubbling with He through an aquarium aerator. We determined K_s with Darcy's equation.

$$K_s = QL/A(H_2 - H_1), \quad (1)$$

where

K_s saturated hydraulic conductivity (cm/s);

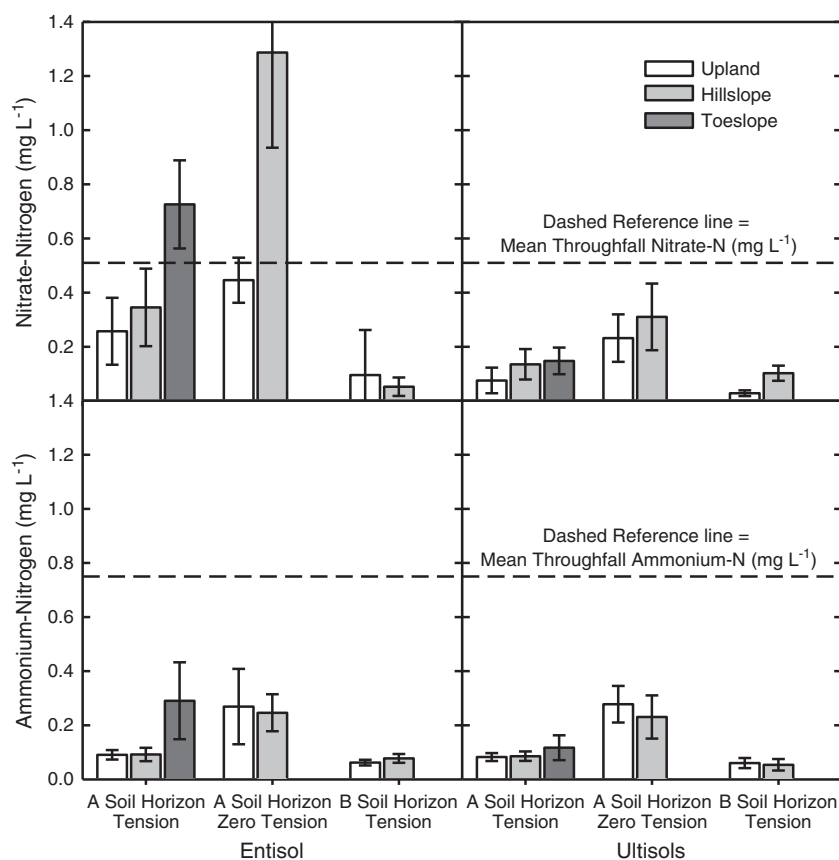


Figure 3. Spatial mean soil solution inorganic N concentrations and standard error sampled during 2009 ($N=4$ for upland and hillslope locations and $N=3$ for toeslope locations). See Table 2 for statistics.

Q volume of water discharged per time (cm^3/s);
 L length of core (cm);
 A cross-sectional area of inner sampling region (cm^2);
 $(H_2 - H_1)$ hydraulic head difference (cm).

[14] Dissolved inorganic N concentrations in lysimeter solutions and throughfall were determined with microplate spectrophotometry. Solid soil sample C and N concentrations and N isotope ratios were determined with an elemental analyzer interfaced to an isotope ratio mass spectrometer. Oxygen isotope ratios were determined from throughfall and lysimeter solutions with a laser water isotope analyzer. All isotope analyses were conducted at the University of California Stable Isotope Facility (Davis, California, USA). Total soil C and N are the means of the five soil core samples from each sample location. Soil texture was determined with the method presented by *Kettler et al.* [2001] on one composite sample derived from the five soil cores at each location. Bulk density was measured for each core using the mass of dry soil ($<2\text{ mm}$) and the volume of the sample.

2.3. Data Analysis

[15] Because we were interested in the effects of soil order, landscape locations, and soil depth on inorganic N concentrations, we calculated the mean inorganic N concentrations for each of the three lysimeter types (shallow TLs, deep TLs, and shallow ZTLs) across sample dates when all lysimeters collected soil solution. All shallow TLs yielded soil solution on 13 sampling occasions, all deep TLs yielded soil solution on 12 occasions, and all

ZTLs yielded soil solution on 10 occasions (supporting information). Therefore, to derive the spatial mean, inorganic N concentrations were first averaged over time within a location (among the above sample occasions) and then averaged across replicate locations (for each soil type, $N=4$ for upland and hillslope and $N=3$ for toeslope).

[16] Data were analyzed with regression and analysis of variance (ANOVA). The ability of SOM properties and K_s to explain variation in lysimeter N concentrations and inorganic N retention was explored with regression analyses. Heteroscedastic data were \log_{10} transformed. Independently, SOM properties, TL and ZTL inorganic N concentrations, 3 day inorganic N retention in unextractable pools, and K_s were analyzed as dependent variables with three-way ANOVA. Lysimeter data were analyzed with an unbalanced three-way ANOVA because we lacked toeslope lysimeters in one of the three transects in each soil type. Soil order and landscape location were analyzed as main plots, and soil depth was treated as a split plot. The interaction between soil depth and landscape location was not analyzed due to the lack of depth sampling at the toeslope location. Soil hydrology (K_s) and ZTL data were analyzed with two-way ANOVA due to the lack of sampling at two soil depths. Soil order and landscape location were treated as main plots.

[17] Oxygen isotope data were used to estimate the transit time (mean residence time) of water sampled in A and B soil horizon TLs [*Dewalle et al.*, 1996; *Maloszewski et al.*, 1983]. A sine wave model was fitted to annual fluctuations in $\delta^{18}\text{O}$ of H_2O in throughfall inputs and lysimeter solutions:

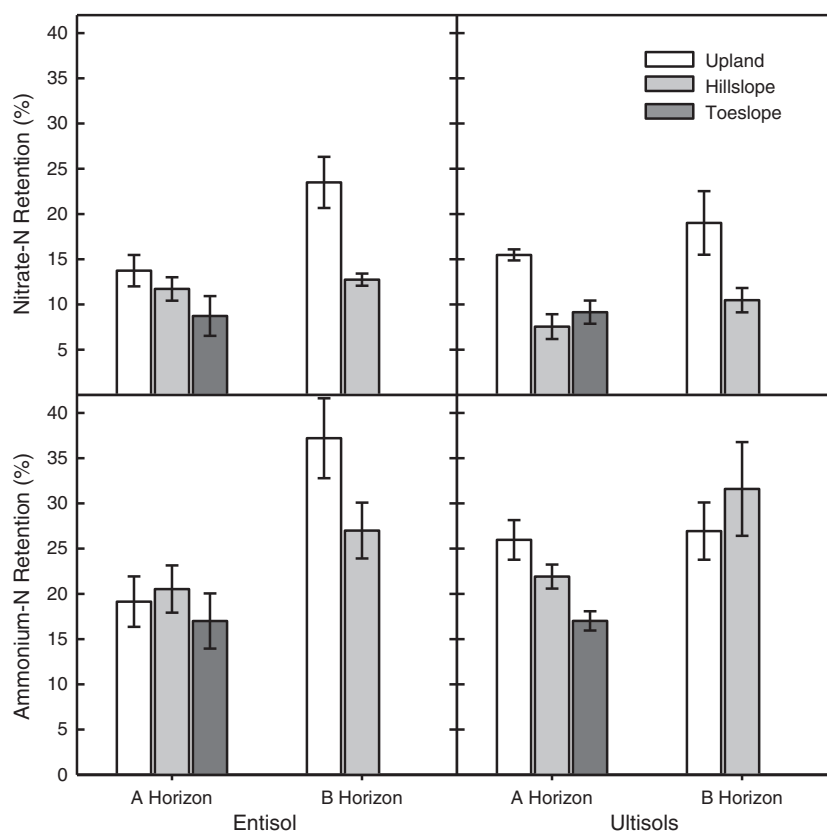


Figure 4. Mean (standard error) fractions of ^{15}N -labeled $\text{NH}_4\text{-N}$ and $\text{NO}_3\text{-N}$ pools that were retained in soil pools not extractable with 2 M KCl after 3 days of in situ incubation ($N=4$). See Table 2 for statistics.

$$\delta^{18}\text{O} = X + A[\cos(ct - \theta)], \quad (2)$$

where $\delta^{18}\text{O}$ is the predicted O isotope ratio in per mil, X is the annual mean $\delta^{18}\text{O}$ in per mil, A is the annual amplitude of $\delta^{18}\text{O}$ in per mil, c is the radial frequency of $\delta^{18}\text{O}$ in radians ($0.017214 \text{ rad d}^{-1}$), t is the time in days after the first water sample (15 December 2008), and θ is the peak annual $\delta^{18}\text{O}$ in radians. Subsequently, the dampening of the annual $\delta^{18}\text{O}$ amplitude in the lysimeter solution sine wave models compared to the annual $\delta^{18}\text{O}$ amplitude in the throughfall solution sine wave model can be used to estimate transit time as

$$T = c^{-1} \left[\frac{A_{z2}}{A_{z1}} \right]^{-2} - 1 \Big]^{0.5}, \quad (3)$$

where T is transit time, c is as defined above, A_{z2} is the amplitude of the lysimeter soil solution model, and A_{z1} is the amplitude of the throughfall sine wave model. Because this method only provides a rough estimate of transit time and all lysimeters did not collect water throughout the 1 year period required for these analyses, we did not calculate unique transit times for each individual lysimeter. Instead, we fitted models to $\delta^{18}\text{O}$ data that were pooled among all replicate lysimeters across soil types for each landscape and soil depth location ($N=8$ lysimeters in A and B soil horizons at upland and hillslope locations and $N=6$ in A horizon lysimeters at toeslope locations). Although we would expect transit time to differ among the soil types due to differences in texture, this modeling approach is not expected to be sufficiently sensitive to accurately characterize small differences in transit time [Dewalle *et al.*, 1996]. Accordingly, we used this approach to explore potential differences in H_2O transit time among the upland, hillslope, and toeslope landscape positions as well as between the A and B soil horizons.

3. Results

[18] Sand content was higher in the Entisol, while silt and clay contents were higher in the Ultisols (Tables 1 and 2). Although bulk density was lower in A horizons (mean = 0.86 g cm^{-3}) than B horizons (mean = 1.08 g cm^{-3}), it did not vary predictably with soil properties or landscape location (data not shown). Accordingly, we report soil C and N per mass of dry soil ($<2 \text{ mm}$). Total SOC and SON were well correlated ($R=0.98$, $p < 0.0001$). Soil type did not have a significant effect on SOC or SON; however, C/N ratio was lower in the sandy Entisol (Figure 2 and Tables 1 and 2). Landscape location had a significant effect on SOC, SON, and C/N ratio (Table 2); all increased downslope (Figure 2).

[19] Inorganic N concentrations in TL samples were greater in the sandy Entisol and increased downslope (Figure 3 and Table 2). Significant interactions between soil type and landscape location indicated that the downslope increase in TL $\text{NH}_4\text{-N}$ and $\text{NO}_3\text{-N}$ concentrations was greater in the sandy Entisol compared to silty Ultisols (Figure 3 and Table 2). Concentrations of $\text{NH}_4\text{-N}$ in ZTLs did not differ among soil types or landscape locations. However, concentrations of $\text{NO}_3\text{-N}$ in ZTLs were greater in the Entisol and increased downslope (Figure 3 and Table 2).

[20] Retention of $^{15}\text{NH}_4\text{-N}$ in SOM during the 3 day in situ incubation was only affected by soil horizon (Table 2).

A greater fraction of the initial $\text{NH}_4\text{-N}$ pool was retained in B horizons versus A horizons (Figure 4). By contrast, retention of $^{15}\text{NO}_3\text{-N}$ during the 3 day incubation was affected by landscape location and soil horizon (Table 2). A greater fraction of the initial $\text{NO}_3\text{-N}$ pool was retained in B horizons, and $\text{NO}_3\text{-N}$ retention decreased downslope in both horizons (Figure 4).

[21] Regression analyses between SOM properties, soil solution inorganic N concentrations, and ^{15}N retention only revealed significant negative correlations between A horizon $^{15}\text{NH}_4\text{-N}$ retention and A horizon SON ($R=-0.70$, $p=0.0002$) and SOC ($R=-0.68$, $p=0.0010$); SOM C/N ratios were not correlated with soil solution inorganic N concentrations or inorganic N retention. However, sand and silt contents were correlated with A horizon $^{15}\text{NH}_4\text{-N}$ retention, soil solution $\text{NO}_3\text{-N}$ concentrations in the A horizon, and K_s . In all cases,

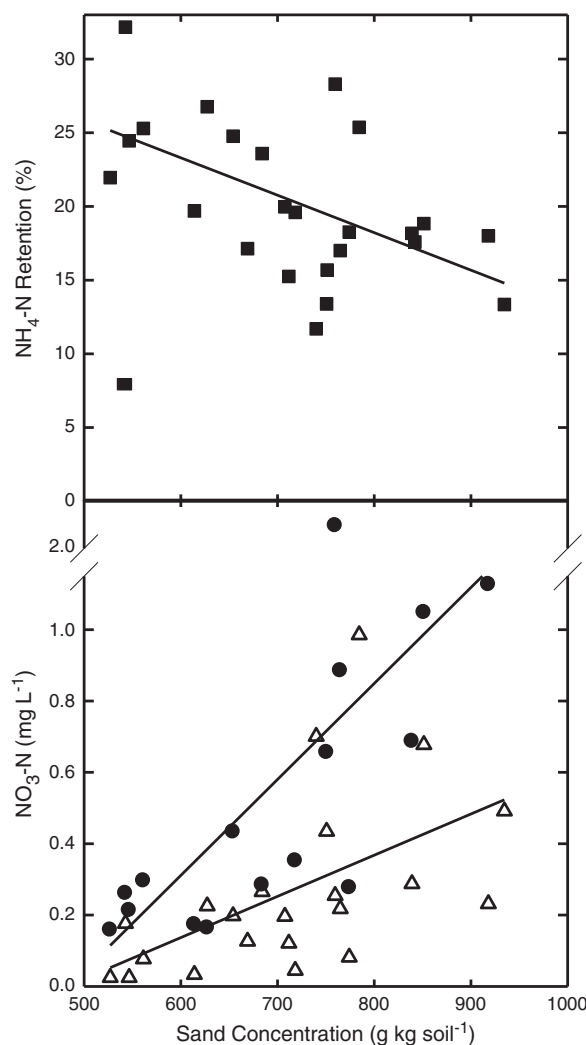


Figure 5. The A soil horizon sand concentration was negatively linearly correlated with A soil horizon $\text{NH}_4\text{-N}$ retention in insoluble pools during a 3 day in situ incubation (black squares; $R=-0.56$, $p=0.0444$). The A soil horizon sand concentration positively linearly correlated with mean annual ZTL $\text{NO}_3\text{-N}$ concentrations (black circles; $R=0.63$, $p=0.0090$) and mean annual A horizon TL $\text{NO}_3\text{-N}$ concentrations (open triangles; $R=0.53$, $p=0.0105$).

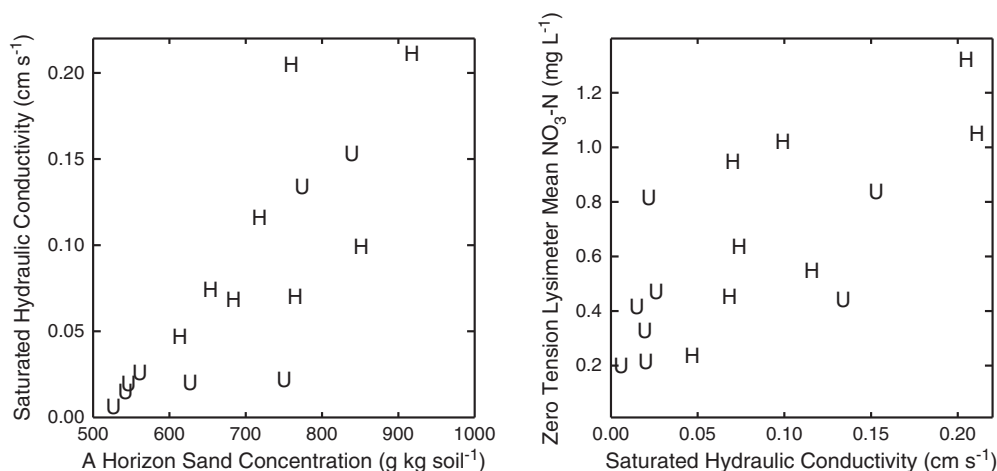


Figure 6. U = Upland; H = Hillslope. Prior to regression analysis, data were \log_{10} transformed to correct for heteroscedasticity. A horizon sand concentration was positively correlated with saturated hydraulic conductivity ($R=0.81$, $p=0.0002$). Saturated hydraulic conductivity was positively correlated with the spatial mean of ZTL $\text{NO}_3\text{-N}$ concentrations ($R=0.61$, $p=0.0116$).

Table 3. Annual $\delta^{18}\text{O}$ (‰) Characteristics of Water Sampled from Throughfall and TLs Used to Parameterize a Soil Solution Transit Time Model

Water Type		Minimum	Maximum	Average	SD ^b	Amplitude	Transit Time
		$\delta^{18}\text{O}$ (‰)					Days
Throughfall		-14.1	-2.3	-7.3	2.9	-11.7	-
A Soil Horizon TL (12–15 cm)	Upland	-11.4	-4.3	-6.5	1.1	-7.2	75
	Hillslope	-9.5	-3.9	-6.5	1.1	-5.6	108
	Toeslope	-8.6	-5.0	-6.6	1.0	-3.6	180
B Soil Horizon TL (85–100 cm)	Upland	-7.9	-5.5	-6.9	0.6	-2.4	276
	Hillslope	-8.0	-5.2	-6.7	0.5	-2.8	237

^aSee equations (2) and (3). Data are displayed in the supporting information.

^bStandard deviation.

correlations with sand were stronger and in the opposite direction of correlations with silt; accordingly, we display correlations with sand only. Variation in clay contents was low (Table 1) and not correlated with any variables. Retention of $^{15}\text{NH}_4\text{-N}$ in A horizon soils was negatively linearly correlated with sand (Figure 5) and positively linearly correlated with silt ($R=0.51$, $p=0.0106$). Soil solution $\text{NO}_3\text{-N}$ concentrations in A horizon TLs and ZTLs were positively correlated with sand (Figure 5) and negatively correlated with silt (TLs: $R=-0.55$, $p=0.0086$; ZTLs: $R=-0.60$, $p=0.0141$). Similarly, K_s was positively correlated with sand (Figure 6) and negatively correlated with silt ($R=-0.76$, $p<0.0006$). $\text{NO}_3\text{-N}$ concentrations in ZTLs were positively correlated with K_s (Figure 6). All correlations with K_s required \log_{10} transformation to reduce heteroscedasticity. Soil type and landscape location had a significant effect on K_s (Table 2); the sandy Entisol had higher K_s than the silty Ultisols, and K_s was greater at the hillslope location compared to the upland location (Figure 6 and Table 2).

[22] Transit time estimates of soil solutions sampled in A horizon TLs increased downslope from 75 days at the upland location to 108 days at the hillslope location and 179 days at the toeslope location. Transit time estimates for B horizon soil solutions were 276 days for the upland location and 237 days for the toeslope location (Table 3 and supporting information).

4. Discussion

4.1. Site Hydrology

[23] Soil hydrology and texture data indicate that downslope water transport occurs through lateral flow within soil horizons as well as vertical flow through soil horizons. The downslope increase in transit time estimates of the A horizon soil solution sampled with TLs (Table 3) is consistent with some downslope lateral flow within the A horizon that may be produced by a longer flow path length to lysimeters at lower elevation locations on the hillslope. Abrupt changes in soil properties at horizon interfaces can promote lateral flow [Lin and Zhou, 2008]; indeed, bulk density was greater in B horizons than A horizons and our lysimeters were placed at the interface of these soil horizons. Steep slopes (20%; Figure 1) may further promote lateral flow. The downslope increase in transit time could not be attributed to lower hydraulic conductivity at downslope locations because K_s increased downslope (Tables 1 and 2).

[24] Although we found no downslope difference in volumetric water contents (unpublished data), this finding may be the result of downslope changes in K_s and texture (Tables 1 and 2). This lack of difference does, however, suggest that differences in SOM decomposition are not responsible for downslope increases in SOC, SON, and NO_3 . Moreover, the concomitant downslope increase in C/N ratios

and NO_3 concentrations suggests NO_3 is not produced locally but transported from upslope. Together, these data suggest connected lateral flow paths through hillslope surface soils are active and lead to a downslope accumulation of materials. Nevertheless, vertical flow through soil horizons to the paleosol with low hydraulic conductivity and subsequent downslope travel are also likely important. Evidence for this process includes visible water flow at the toeslope seep where the paleosol interfaces with the surface soil (supporting information). Lower hydraulic conductivity and longer vertical flow paths to B horizon lysimeters compared to A horizon lysimeters may cause the longer soil solution transit times to B horizon lysimeters (Table 3). Although we did not measure K_s in the B horizon, greater bulk density in B horizon soils suggests that K_s may be lower in B versus A horizons. It is not clear why transit times were longer in upland B horizons than hillslope B horizons (Table 3).

4.2. Nitrogen Dynamics Along the Slope

[25] Our results suggest hydrological flow paths and soil type interact to modulate N saturation symptoms, including soil solution NO_3 concentrations and NO_3 retention in SOM. Soil solution NO_3 concentrations increased downslope, while $^{15}\text{NO}_3\text{-N}$ retention decreased downslope (Figures 2 and 3). The downslope increase in soil solution NO_3 in ZTL samples, which incorporated the effects of periodic advective transport, was greater in the sandy Entisol with greater K_s than the silty Ultisols (Figure 2 and Table 2). By contrast, we found relatively few effects of soil type, hillslope location, or their interaction on measures of N saturation that did not incorporate advective processes; there was no effect of soil type on $^{15}\text{NH}_4$ or $^{15}\text{NO}_3$ retention in SOM (Figure 4 and Table 2). Accordingly, the intense periodic advective NO_3 transport that was captured by ZTL sampling appears to be an important contributor to downslope and subsoil biogeochemistry. Across all sampling locations, higher NO_3 concentrations in ZTLs compared to TLs indicate that biological N demand is not completely saturated at any sampling location, affirming the dual importance of periodic transport and biological N immobilization. However, higher K_s , lower $^{15}\text{NH}_4\text{-N}$ retention, and higher NO_3 concentrations in sandy soils (Figures 5 and 6) indicate differences in hydrology, and N retention kinetics account for greater variation in N dynamics than biological demand.

[26] Our results provide important contrasts with previous N saturation research that focused on biological demand and demonstrated positive correlations among SOC, C/N ratios, and N retention as well as negative correlations among SOC, C/N ratios, and soil solution NO_3 [Emmett *et al.*, 1998; Evans *et al.*, 2006; Lovett *et al.*, 2002]. At our site, the downslope increase in soil solution NO_3 concentrations and decrease in NO_3 retention occurred concomitantly with a downslope increase in SOC and C/N ratios (Figures 2–4 and Table 2). We suggest inorganic N inputs via lateral hillslope flow paths may overwhelm the positive effects of increasing SOC and C/N ratios on downslope inorganic N retention. The established relationship between C/N ratios and N saturation symptoms is highly variable within the range of C/N ratios at our site [Ross *et al.*, 2009], and soil hydrology may be one factor contributing to the variation.

[27] Several processes could have contributed to increasing downslope SOC and SON concentrations, including

microclimate, soil physical properties, and an accumulation of dissolved C and N inputs from upslope. However, research focusing on vertical soil water flow paths has determined that dissolved OM (DOM) transport from surface soils is an important source of subsoil SOM accumulation [Marin-Spiotta *et al.*, 2011; Sanderman and Amundson, 2008]. Similarly, significant portions of surface soil inorganic N production can be retained in subsoils after transformation to SON [Dittman *et al.*, 2007; Huygens *et al.*, 2008]. Soil solution data from TLs confirm subsoils are an important sink for inorganic N at our site: the mean $\text{NO}_3\text{-N}$ decrease from A to B soil horizons was 50% (Figure 2). Furthermore, our ^{15}N retention measurements suggest that the decrease can be explained by $\text{NO}_3\text{-N}$ transfer to insoluble SOM (Figure 3). Although we cannot determine the importance of downslope lateral flow in the A horizon, the downslope increase in SOC, SON, and NO_3 concentrations is consistent with lateral hydrological transport downslope.

[28] Consistent with SOM saturation theory [Six *et al.*, 2002], increasing downslope SOC and SON concentrations could be the result of long-term DOM inputs from upslope locations that concomitantly increase downslope SOM pools and decrease downslope N retention. Although the downslope decrease in $^{15}\text{NO}_3$ retention and increase in SON concentrations may appear inconsistent, the efficiency of dissolved organic C and N retention in insoluble SOM can decrease with increasing SOM C and SOM N concentrations [Castellano *et al.*, 2012; Stewart *et al.*, 2007] and much of the inorganic N retention in insoluble SOM occurs after biological transformation to dissolved organic N and subsequent adsorption to solid particles [Norton and Firestone, 1996; Sollins *et al.*, 1996; Zogg *et al.*, 2000].

4.3. Nitrogen Dynamics in Contrasting Soil Types

[29] There is no consistent relationship between soil texture and N cycling. For example, sand content, N mineralization, and dissolved NO_3 fluxes have been reported to be positively, negatively, or not correlated [Bechtold and Naiman, 2006; Cote *et al.*, 2000; Giardina *et al.*, 2001; Gu and Riley, 2010; Pastor *et al.*, 1984; Reich *et al.*, 1997]. Positive correlations between sand, N mineralization, and N fluxes may be the result of lower potential N stabilization in silt-associated and clay-associated SOM. Negative correlations may be the result of soil texture effects on water content. Sandy soils typically have low water holding capacity, and water content is a key control on C and N dynamics [Castellano *et al.*, 2011]. Moreover, the relationship between soil texture and N cycling is often confounded by differences in vegetation biochemistry [Mueller *et al.*, 2012; Pastor *et al.*, 1984; Reich *et al.*, 1997], a variable that was controlled at our site.

[30] Recent research suggests that the inconsistent relationship between soil texture and N cycling may be reconciled by focusing on the capacity for silt and clay particles to stabilize SOM [Castellano *et al.*, 2012]. Soils with a large capacity for SOM stabilization in silt+clay fractions, regardless of texture, may exhibit high inorganic N retention and low N mineralization. The capacity for SOM stabilization in silt+clay fractions is a function of silt+clay contents as well as cumulative OM inputs [Hassink, 1997]. The unoccupied capacity for SOM stabilization by silt+clay

particles can be described as the SOM or SOC “saturation deficit” [Stewart *et al.*, 2007].

[31] At our site, the negative relationships among sand, SOM, and $^{15}\text{NH}_4\text{-N}$ retention in SOM, coupled with the positive correlation between sand content and soil solution NO_3 concentrations (Figure 6), suggest mineral-protected pools in sandy soils have lower N retention kinetics that result in lower microbial N demand and higher NO_3 concentrations. During intense precipitation events that produced rapid advective soil solution transport, high K_s in sandy soils appears to promote flushing of NO_3 that has accumulated due to low retention (Figures 5 and 6). Positive correlations between K_s and ZTL NO_3 concentrations suggest that increasing soil solution transport rates decrease NO_3 retention in SOM. These data are consistent with NO_3 flushing concepts [Creed and Band, 1998; van Verseveld *et al.*, 2008] and contribute to the biological understanding of NO_3 flushing processes.

5. Conclusions

[32] Explaining why ecosystems vary in how quickly they reach N saturation remains an important challenge. Recent conceptual models suggest that the time to onset of N saturation symptoms is a function of N uptake capacity and kinetics [Lovett and Goodale, 2011]. Our results suggest that the rate at which an ecosystem retains N (kinetics), the rate at which an ecosystem transports N, and the total amount of N it can retain (capacity) are functions of SOM properties and hydraulic conductivity, which are regulated in turn by soil texture. We demonstrate that a downslope increase in NO_3 concentrations is coincident with a downslope decrease in inorganic N retention capacity (Figures 2 and 3). We hypothesize that downslope transport of dissolved C and N contributes to this observation. If widespread, this pattern can help account for the variability in watershed NO_3 export. Indeed, a recent study of nine watersheds in the northeastern United States demonstrated that a topographic index (tangent of upslope area/slope) was positively correlated with NO_3 export, while the ability of potential nitrification rates to explain variation in watershed NO_3 export was significantly improved when data were limited to downslope soils near the stream and watershed outlet [Ross *et al.*, 2012].

[33] As N inputs accumulate, soil texture can impact the kinetics and capacity of N retention. In ecosystems with sandy soils, N retention is often low [Lajtha *et al.*, 1995; Pregitzer *et al.*, 2004]. We link this observation to hydrological and physicochemical mechanisms that affect N retention kinetics and capacity. The potential rate of dissolved N transport (K_s) was positively correlated with soil solution NO_3 concentrations (Figure 4), while NO_3 retention was lower and NO_3 concentrations were higher in soils with a low capacity for physicochemical SOM N protection by association with silt and clay particles (Figures 2 and 3).

[34] The effects of soil texture on N retention may be difficult to observe in ecosystems with low SOM or rapid biomass accumulation rates because N sinks should efficiently retain large N inputs [Castellano *et al.*, 2012; Vitousek and Reiners, 1975]. However, as the capacity for N retention decreases, so should the kinetics of N retention. These results may help explain the variation in the NO_3 flushing pattern, which is not universally observed [Hill *et al.*,

1999]. In watersheds where the NO_3 flushing pattern is absent, the N retention capacity should be relatively large with rapid kinetics. Alternatively, in watersheds where NO_3 flushing is manifest as a result of rapid NO_3 transport from surface soils, the N retention capacity should be low, thereby decreasing N retention kinetics that can mitigate NO_3 loss during rapid soil water flow.

[35] Advances in N saturation and retention theories have focused on surface soil N biogeochemistry in the absence of dynamic soil hydrology. Our results reveal important gaps in N retention theory based on soil biogeochemistry alone and demonstrate how microbial and hydrological processes can interact to affect N dynamics. Recent numerical models of N dynamics that incorporate microbial processes as well as advective transport offer an excellent framework to interpret the relative importance of biological and hydrological controls on the expression of N saturation symptoms [Gu and Riley, 2010; Maggi *et al.*, 2008]. These models distinguish between kinetic and capacity N saturation processes and have the potential to explain patterns in our data that are coincident with N inputs, hydrology, and SOM stabilization capacity. In soils with coarse texture, low capacity for physicochemical SOM N protection by association with silt and clay particles (capacity saturation) may feedback with rapid advective N transport (kinetic saturation) to hasten the expression of ecosystem N saturation symptoms. Field studies paired with models offer an approach to explore the transferability and relative importance of these processes to ecosystems beyond the catchment studied herein.

[36] **Acknowledgments.** Dennis Lock provided statistical advice and programming. This project was funded by NSF (DEB Dissertation Improvement Grant 090999) and NOAA (National Estuarine Research Reserve Graduate Research Fellowship program) (to M.J.C.). J.P.K. was funded by NSF DEB 0816668. M.J.C. was funded by USDA (National Needs 2005-38420-15774).

References

- Aber, J., K. Nadelhoffer, P. Steudler, and J. M. Melillo (1989), Nitrogen saturation in northern forest ecosystems, *Bioscience*, *39*, 378–386.
- Bechtold, S. J., and R. J. Naiman (2006), Soil texture and nitrogen mineralization potential across a riparian toposequence in a semi-arid savanna, *Soil Biology and Biochemistry*, *38*(6), 1325–1333, doi:10.1016/j.soilbio.2005.09.028.
- Castellano, M. J., J. P. Kaye, H. Lin, and J. P. Schmidt (2012), Linking Carbon Saturation Concepts to Nitrogen Saturation and Retention, *Ecosystems*, doi:10.1007/s10021-011-9501-3.
- Castellano, M. J., J. P. Schmidt, J. P. Kaye, C. Walker, C. B. Graham, H. Lin, and C. Dell (2011), Hydrological controls on heterotrophic soil respiration across an agricultural landscape, *Geoderma*, *16*, 273–280, doi:10.1016/j.geoderma.2011.01.020.
- Cote, L., S. Brown, D. Pare, J. Fyles, and J. Bauhus (2000), Dynamics of carbon and nitrogen mineralization in relation to stand type, stand age and soil texture in the boreal mixedwood, *Soil Biology and Biochemistry*, *32*, 1079–1090.
- Creed, I. F., and L. E. Band (1998), Export of nitrogen from catchments within a temperate forest: Evidence for a unifying mechanism regulated by variable source area dynamics, *Water Resour.*, *34*(11), 3105–3120.
- Dewalle, D. R., P. J. Edwards, B. R. Swistock, R. Aravena, and R. J. Drimmie (1997), Seasonal isotope hydrology of three appalachian forest catchments, *Journal of Hydrology*, *11*(1996), 1895–1906.
- Dittman, J. A., C. T. Driscoll, P. M. Groffman, and T. J. Fahey (2007), Dynamics of nitrogen and dissolved organic carbon at the Hubbard brook experimental forest, *Ecology*, *88*(5), 1153–66.
- Emmett, B. A. (2007), Nitrogen Saturation of Terrestrial Ecosystems: Some Recent Findings and Their Implications for Our Conceptual Framework, *Water, Air, & Soil Pollution: Focus*, *7*, 99–109, doi:10.1007/s11267-006-9103-9.

- Emmett, B. A., D. Boxman, M. Bredemeier, P. Gundersen, O. J. Kjønaas, F. Moldan, P. Schleppi, A. Tietema, and R. F. Wright (1998), Predicting the Effects of Atmospheric Nitrogen Deposition in Conifer Stands: Evidence from the NITREX Ecosystem-Scale Experiments, *Ecosystems*, 1, 352–360.
- Evans, C. D., et al. (2006), Evidence that Soil Carbon Pool Determines Susceptibility of Semi-Natural Ecosystems to Elevated Nitrogen Leaching, *Ecosystems*, 9(3), 453–462, doi:10.1007/s10021-006-0051-z.
- Evans, C. D., D. Norris, N. Ostle, H. Grant, E. C. Rowe, C. J. Curtis, and B. Reynolds (2008), Rapid immobilisation and leaching of wet-deposited nitrate in upland organic soils, *Environ. Pollut.*, 156, 636–643, doi:10.1016/j.envpol.2008.06.019.
- Giardina, C. P., M. G. Ryan, R. M. Hubbard, D. Binkley, and F. E. For (2001), Tree Species and Soil Textural Controls on Carbon and Nitrogen Mineralization Rates, *Soil Science Society of America Journal*, 65, 1272–1279.
- Gu, C., and W. J. Riley (2010), Combined effects of short term rainfall patterns and soil texture on soil nitrogen cycling - a modeling analysis, *J. Contam. Hydrol.*, 112(1-4), 141–54, doi:10.1016/j.jconhyd.2009.12.003.
- Hassink, J. (1997), The capacity of soils to preserve organic C and N by their association with clay and silt particles, *Plant and Soil*, 191, 77–87.
- Hill, A. R., W. A. Kemp, J. M. Buttle, and D. Goodyear (1999), Nitrogen chemistry of subsurface storm runoff on forested Canadian Shield hillslopes, *Water Resour.*, 35(3), 811–821.
- Huygens, D., P. Boeckx, P. Templer, L. Paulino, O. Van Cleemput, C. Oyarzún, C. Müller, and R. Godoy (2008), Mechanisms for retention of bioavailable nitrogen in volcanic rainforest soils, *Nat. Geosci.*, 1(8), 543–548, doi:10.1038/ngeo252.
- Kaye, J., J. Barrett, and I. Burke (2002), Stable Nitrogen and Carbon Pools in Grassland Soils of Variable Texture and Carbon Content, *Ecosystems*, 5, 461–471, doi:10.1007/s10021-002-142-4.
- Kettler, T. A., J. W. Doran, and T. L. Gilbert (2001), Simplified Method for Soil Particle-Size Determination to Accompany Soil-Quality Analyses, *Soil Science Society of America Journal*, 65, 849–852.
- Klute, A., and C. Dirksen (1986), Hydraulic conductivity and diffusivity: laboratory methods, in *Methods of soil analysis: Part I - Physical and Mineralogical Methods*, edited by A. Klute, p. 687–734.
- Lajtha, K., B. Seely, and I. Valiela (1995), Retention and leaching losses of atmospherically-derived nitrogen in the aggrading coastal watershed of Waquoit Bay, MA, *Biogeochemistry*, 28, 33–54.
- Lewis, D. B., and J. P. Kaye (2011), Inorganic nitrogen immobilization in live and sterile soil of old-growth conifer and hardwood forests: implications for ecosystem nitrogen retention, *Biogeochemistry*, doi:10.1007/s10533-011-9627-6.
- Lin, H., and X. Zhou (2008), Evidence of subsurface preferential flow using soil hydrologic monitoring in the Shale Hills catchment, *European Journal of Soil Science*, 59(1), 34–49, doi:10.1111/j.1365-2389.2007.00988.x.
- Lovett, G. M., and C. L. Goodale (2011), A new conceptual model of nitrogen saturation based on experimental nitrogen addition to an oak forest, *Ecosystems*, 14(4), 615–631, doi:10.1007/s10021-011-9432-z.
- Lovett, G. M., K. C. Weathers, and M. A. Arthur (2002), Control of nitrogen loss from forested watersheds by soil carbon:nitrogen ratio and tree Species Composition, *Ecosystems*, 5(7), 712–718, doi:10.1007/s10021-002-0153-1.
- Lovett, G. M., K. C. Weathers, and W. V. Sobczak (2000), Nitrogen saturation and retention in forested watersheds of the Catskill Mountains, New York, *Ecol. Appl.*, 10, 73–84.
- Maggi, F., C. Gu, W. J. Riley, G. M. Hornberger, R. T. Venterea, T. Xu, N. Spycher, C. Steefel, N. L. Miller, and C. M. Oldenburg (2008), A mechanistic treatment of the dominant soil nitrogen cycling processes: Model development, testing, and application, *J. Geophys. Res.*, 113(G2), 1–13, doi:10.1029/2007JG000578.
- Magill, A. H., J. D. Aber, G. M. Berntson, W. H. McDowell, K. J. Nadelhoffer, J. M. Melillo, and P. Steudler (2000), Long-Term Nitrogen Additions and Nitrogen Saturation in Two Temperate Forests, *Ecosystems*, 3(3), 238–253, doi:10.1007/s100210000023.
- Maloszewski, P., W. Rauert, W. Stichler, and A. Herrmann (1983), Application of flow models in an alpine catchment area using tritium and deuterium data, *Journal of Hydrology*, 66, 319–330.
- Marin-Spiotta, E., O. A. Chadwick, M. Kramer, and M. S. Carbone (2011), Carbon delivery to deep mineral horizons in Hawaiian rain forest soils, *J. Geophys. Res.*, 116(G3), 1–14, doi:10.1029/2010JG001587.
- Mitchell, M. J. (2001), Linkages of nitrate losses in watersheds to hydrological processes, *Hydrological Processes*, 15(17), 3305–3307, doi:10.1002/hyp.503.
- Mueller, K. E., S. E. Hobbie, J. Oleksyn, P. B. Reich, and D. M. Eissenstat (2012), Do evergreen and deciduous trees have different effects on net N mineralization in soil?, *Ecology*, 93, 1463–72.
- Norton, M., and M. K. Firestone (1996), N Dynamics in the rhizosphere of Pinus Ponderosa Seedlings, *Soil Biology and Biochemistry*, 28, 351–362.
- Pastor, J., J. D. Aber, C. A. McLaugherty, and J. M. Melillo (1984), Above-ground production and N and P cycling along a nitrogen mineralization gradient on Blackhawk Island, Wisconsin, *Ecology*, 65, 256–268.
- Pionke, H. B., W. J. Gburek, A. N. Sharpley, and R. R. Schnabel (1996), Flow and nutrient export patterns for an agricultural, *Water Resour.*, 32(6), 1795–1804.
- Pregitzer, K. S., D. R. Zak, J. Andrew, J. A. Ashby, and N. W. Macdonald (2004), Chronic nitrate additions dramatically increase the export of carbon and nitrogen from northern hardwood ecosystems, *Biogeochemistry*, 68, 179–197.
- Reich, P., D. Grigal, J. Aber, and S. T. Gower (1997), Nitrogen mineralization and productivity in 50 hardwood and conifer stands on diverse soils, *Ecology*, 78(2), 335–347.
- Ross, D. S., J. B. Shanley, J. L. Campbell, G. B. Lawrence, S. W. Bailey, G. E. Likens, B. C. Wemple, G. Fredriksen, and A. E. Jamison (2012), Spatial patterns of soil nitrification and nitrate export from forested headwaters in the northeastern United States, *J. Geophys. Res.*, 117(G1), 1–14, doi:10.1029/2011JG001740.
- Ross, D. S., B. C. Wemple, A. E. Jamison, G. Fredriksen, J. B. Shanley, G. B. Lawrence, S. W. Bailey, and J. L. Campbell (2009), A Cross-Site Comparison of Factors Influencing Soil Nitrification Rates in Northeastern USA Forested Watersheds, *Ecosystems*, 12(1), 158–178, doi:10.1007/s10021-008-9214-4.
- Sanderman, J., and R. Amundson (2008), A comparative study of dissolved organic carbon transport and stabilization in California forest and grassland soils, *Biogeochemistry*, 92(1-2), 41–59, doi:10.1007/s10533-008-9249-9.
- Schlesinger, W. H. (2009), On the fate of anthropogenic nitrogen, *Proc. Natl. Acad. Sci. U. S. A.*, 106(1), 203–8, doi:10.1073/pnas.0810193105.
- Six, J., R. T. Conant, E. A. Paul, and K. Paustian (2002), Stabilization mechanisms of soil organic matter: Implications for C-saturation of soils, *Plant and Soil*, 241, 155–176.
- Sollins, P., P. Homann, and B. A. Caldwell (1996), Stabilization and destabilization of soil organic matter: mechanisms and controls, *Geoderma*, 74, 65–105.
- Stewart, C. E., K. Paustian, R. T. Conant, A. F. Plante, and J. Six (2007), Soil carbon saturation: concept, evidence and evaluation, *Biogeochemistry*, 86(1), 19–31, doi:10.1007/s10533-007-9140-0.
- van Verseveld, W. J., J. J. McDonnell, and K. Lajtha (2008), A mechanistic assessment of nutrient flushing at the catchment scale, *Journal of Hydrology*, 358(3-4), 268–287, doi:10.1016/j.jhydrol.2008.06.009.
- Vitousek, P. M., and W. A. Reiners (1975), Ecosystem Succession and Nutrient Retention: A Hypothesis, *Bioscience*, 25, 376–381.
- Walker, C., and H. S. Lin (2008), Soil property changes after four decades of wastewater irrigation: A landscape perspective, *Catena* 73, 63–74.
- Zogg, G. P., D. R. Zak, K. S. Pregitzer, and A. J. Burton (2000), Microbial immobilization and the retention of anthropogenic nitrate in a northern hardwood forest, *Ecology*, 81, 1858–1866.